Bonding in Liquid Carbon Studied by Time-Resolved X-Ray Absorption Spectroscopy

S. L. Johnson,[1,2,*] P. A. Heimann,[3] A. G. MacPhee,[1] A. M. Lindenberg,[1,†] O. R. Monteiro,[3] Z. Chang,[4] R. W. Lee,[5] and R. W. Falcone[1,3]

[1]*Department of Physics, University of California, Berkeley, California 94720, USA*
[2]*Paul Scherrer Institut, CH-5232 Villigen PSI, Switzerland*
[3]*Lawrence Berkeley National Laboratory, Berkeley, California 94720, USA*
[4]*Department of Physics, Kansas State University, Manhattan, Kansas 66506, USA*
[5]*Lawrence Livermore National Laboratory, Livermore, California 94551, USA*

(Received 14 April 2004; published 10 February 2005)

Even the most basic properties of liquid carbon have long been debated due to the challenge of studying the material at the required high temperature and pressure. Liquid carbon is volatile and thus inherently transient in an unconstrained environment. In this paper we use a new technique of picosecond time-resolved x-ray absorption spectroscopy to study the bonding of liquid carbon at densities near that of the solid. As the density of the liquid increases, we see a change from predominantly sp-bonded atomic sites to a mixture of sp, sp^2, and sp^3 sites and compare these observations with molecular dynamics simulations.

DOI: 10.1103/PhysRevLett.94.057407 PACS numbers: 78.70.Dm, 61.20.Ne, 64.70.Dv, 71.22.+i

Although considerable attention has been focused on solid forms of carbon, the properties of liquid carbon are much more difficult to measure accurately. Liquid carbon may exist as a thermodynamically stable phase near the cores of Uranus and Neptune, contributing to the magnetic moment of these planets [1]. Much of the difficulty encountered in experimental studies is related to the high temperatures (above 5000 K) required, conditions that are difficult to maintain under laboratory conditions. Consequently, experiments have relied on pulsed heating and measurement of a transient liquid phase. These have produced a significant spread in reported properties. For example, although the most recent and reliable measurements show liquid carbon is metallic [2], reported conductivity values vary by more than an order of magnitude. This variation may be due to a strong dependence of the liquid properties on the temperature and density [3], but so far no one experiment has made such a relationship clear.

In addition to experiments, Wu *et al.* [4] used first-principles molecular dynamics (MD) simulations to explore the properties of the liquid as function of temperature and density. The results suggest that the local bonding structure of the liquid varies continuously as the density increases. At a density of 1.27 g/cm^3, the liquid is a mixture of twofold and threefold coordinated atoms. The liquid passes through a region of primarily threefold coordination at intermediate densities, and at 3.02 g/cm^3 the simulations show that fourfold coordination in the melt becomes significant as the average coordination number reaches 3.4. These results are consistent with computationally simpler tight-binding simulations at 7000 K [5]. This strong dependence of the local structure on density is an intriguing result that encourages experimental investigation.

To study the bonding properties of liquid carbon at near-solid densities, we employed the femtosecond laser pump, x-ray probe technique described in [6]. Initially, the samples under study are 500 Å thick foils of amorphous carbon. An intense 150 fs, 800 nm laser pulse heats the sample, causing it to melt. To probe the state of the resulting liquid in the short time before it vaporizes or breaks up, a 70 ps long, spectrally broad x-ray pulse from a synchrotron bend magnet passes through the liquid. A dispersive grating spectrograph then measures the absorption spectrum near the carbon K edge with a resolution of approximately 3.5 eV. Higher-order grating reflections are suppressed by inserting a pair of parallel, grazing incidence chromium-coated mirrors into the x-ray path before the sample. The mirrors, each at an incidence angle of 4.5°, absorb photon energies above 500 eV. By varying the relative timing of the x-ray and laser pulses, we probe the (nearly instantaneous) melting process and the subsequent expansion dynamics of the liquid with 70 ps resolution.

These expansion dynamics pose a challenge to the experiment. Studies using optical interferometry have estimated the surface expansion velocity from femtosecond ablation to be as high as 1000 m/s [7]. This would seem to imply that a time resolution of approximately 5 ps or better is required to probe the liquid carbon at near its initial density, and indeed one approach pursued in this report is to use an ultrafast x-ray streak camera to measure the x-ray transmission with this level of temporal resolution. Another approach that avoids the experimental complexity of the streak camera is to delay the expansion dynamics of the foil by coating each side with thick layers of LiF, a method of sample preparation called "tamping." The large 14 eV optical band gap of LiF makes this material essentially transparent to the laser even at high fluences, and the mechanical stiffness of the tamping layers prevents the foil from expanding on a time scale $\tau \geq 2d/v \approx 100$ ps, where $d = 3500$ Å is the tamping layer thickness and v is the speed of sound in LiF (approximately 7000 m/s).

This expansion delay allows us to observe the liquid at a density very near that of the initial solid.

We performed pump-probe measurements on three distinct types of solid target foils: (a) 500 Å thick "untamped" (i.e., uncoated) films of amorphous carbon (a-C) with a density of 2.0 g/cm^3 prepared by evaporation from an arc source, (b) 500 Å thick tamped films of electron beam evaporated a-C (also 2.0 g/cm^3), and (c) 500 Å thick tamped films of diamondlike carbon (DLC) with a density of 2.6 g/cm^3 prepared by the filtered cathodic arc technique described in [8] without an electrical bias on the substrate. Figure 1 shows the unheated, solid spectrum for the a-C and DLC foils, and Fig. 2 shows the corresponding liquid spectra 100 ps after heating. For the tamped foils, the smooth LiF background absorption has been subtracted out. The unheated tamped a-C foil spectrum is not shown because it is not significantly different from that of the unheated, untamped a-C foil. The liquid spectra all show large differences from those of the solids, particularly at the preedge resonance near 285 eV.

To ensure that the probed region of each foil was completely melted by the laser, we measured the dependence of the observed spectral changes on the incident laser fluence. In each case, the magnitude of the observed changes reaches a saturation level, where excitation by higher fluences does not further alter the spectra. For the untamped foil, this saturation fluence is 0.7 J/cm^2; for the tamped a-C and DLC foils, the saturation fluences are both about 2 J/cm^2. This behavior in the untamped foil is consistent with earlier fluence-dependence measurements of the size of the ablation craters left behind by femtosecond laser melting of bulk graphite, where the size of the craters increases only very slowly as the average fluence increases beyond 0.7 J/cm^2 [9]. Optical self-absorption measurements using an integrating sphere show that all the foils absorb a similar fraction of the laser energy: for the untamped a-C and tamped DLC foils about 40% is absorbed at these fluences, and for the tamped a-C we estimate 60% absorption (due to a reduced reflectivity). The spectra depicted in Fig. 2 were all taken at excitation fluences above the saturation levels.

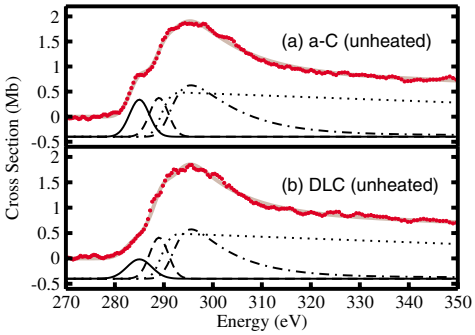

FIG. 1 (color online). K-edge absorption spectra of unheated carbon foils: (a) a-C and (b) DLC (tamped, but after subtracting out LiF background). The solid circles are the data. The smooth curves on the plots show the fit results discussed in the text. Solid black: π^*; dashed: σ_x^*; dash-dotted: σ_c^*; dotted: continuum step; broad gray: sum of fit components.

The spectrum of the untamped liquid does not change measurably with time until approximately 100 ns after heating. At this time the overall absorption decreases due to hydrodynamic transport of the liquid out of the x-ray probe volume, similar to what was observed for silicon foils [6]. The tamped foil data at 100 ps is not significantly different from data at delays of up to 300 ps, suggesting that the tamping layers successfully confine the liquid to nearly its initial volume on these time scales. At longer times (ca. 100 ns) the tamped foils also showed an overall drop in absorption similar to that observed in the untamped foils. Because of time constraints, no spectra were taken of the tamped foils at intermediate time scales.

As a further check of the tamping technique, we measured spectra of untamped a-C foils using an ultrafast x-ray streak camera to obtain 5 ps resolution of the melting process. Figure 3 shows the K-edge spectrum integrated in time from 5–10 ps after melting, comparing it to the tamped a-C foil spectrum at 100 ps after heating. The spectra are strikingly similar, allowing for the slightly more coarse spectral resolution obtained with the streak camera. This confirms that the density of the tamped samples is preserved during the observation time.

The near-edge structure of the carbon K edge has a body of well established literature that assigns various features to π^* and σ^* antibonding states. Specifically, the preedge absorption near 285 eV is due to low-energy bound π^* states [10,11]. The strong increase in absorption at this energy upon melting indicates an increase in the amount of

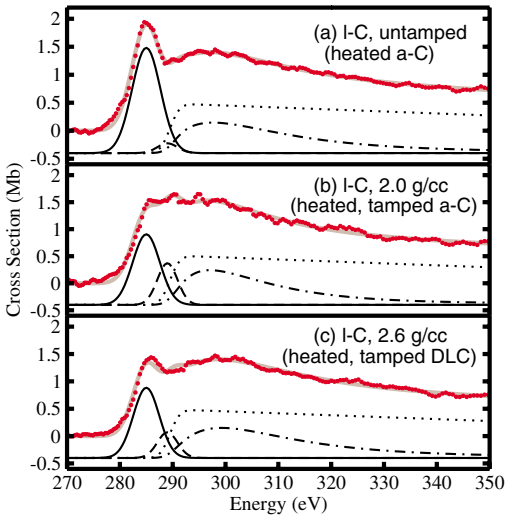

FIG. 2 (color online). K-edge absorption spectra of carbon foils 100 ps after heating: (a) low-density l-C (untamped a-C, incident fluence 2.4 J/cm^2), (b) 2.0 g/cm^3 l-C (tamped a-C, incident fluence 2.1 J/cm^2), and (c) 2.6 g/cm^3 l-C (tamped DLC, incident fluence 2.1 J/cm^2). The solid circles are the data points. For the tamped foils, the LiF background absorption has been subtracted out. The smooth curves show the fit results as in Fig. 1.

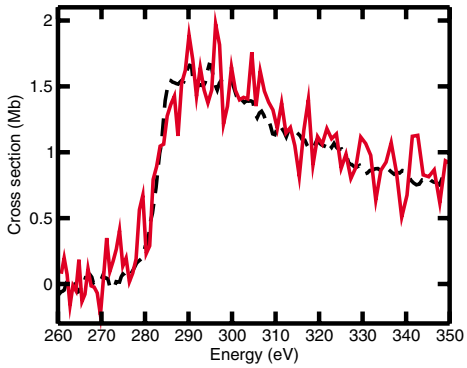

FIG. 3 (color online). Comparison of the spectrum of an untamped a-C foil 5–10 ps after heating to that of a tamped a-C foil 100 ps after heating. Solid line: absorption spectrum from heated a-C obtained using the streak camera detector, integrating in time from 5–10 ps after excitation. Dashed line: tamped a-C spectrum from Fig. 2(b).

π bonding in the material. The much broader absorption near 300 eV is from transitions to σ^* continuum states, and so the decrease in absorption here indicates a lower density of the associated σ bonds. The liquid data also show a blueshift of absorption at these σ^* resonances, an indication of bond length shortening that suggests stronger interaction between carbon atoms.

To extract a quantitative picture of the bonding changes, we use a peak fitting analysis similar to that applied to high-resolution spectra of a-C in [10]. Figures 1 and 2 show the results as curves superimposed on the data. Each spectrum is modeled as the sum of four components. One component, representing π^* states, is a variable-width Gaussian fixed at 285 eV. The continuum step is represented as an error function step with a width of 3.5 eV fixed at 289.5 eV. To model the gradual drop in absorption as the energy increases far above the edge, this continuum step is multiplied by a linear function of energy set to match the observed cross section at 350–450 eV, where all the forms of carbon showed nearly identical absorption. The σ^* continuum states are represented as an asymmetric peak we call σ_c^*. The line shape of σ_c^*, derived in [12], is a three-parameter function of energy that represents the asymmetric absorption cross section expected from a clustered distribution of σ bonds with different lengths. The fourth and final peak is a Gaussian fixed at 289 eV and with a 4.5 eV FWHM. This peak (called σ_x^*) is necessary to obtain acceptable fits of the solid and tamped liquid spectra. The magnitude of this peak is in fact the main difference between the 2.0 and 2.6 g/cm^3 tamped liquid spectra. The physical meaning of this feature is unfortunately ambiguous, since the energy position could correspond to non-continuum σ^* states or to conjugated π^* states (as seen in C_{60} and benzene [13,14]). The fits of solid a-C in [10] also required a peak at approximately the same energy, and the authors attributed the feature to σ^* states on the basis of its behavior upon annealing of the a-C samples. For this reason we tentatively assign this peak to σ^* states.

The magnitude of the π^* absorption indicates the average number of π bonded electrons per atom. Following the reasoning presented in Ref. [10], we can estimate the relative number of π^* states in each form of carbon by taking the area under the π^* peak. To transform these relative areas into an estimated number of π^* states/atom, we use the spectrum of C_{60} from [13] as a reference [15]. Since C_{60} is a purely sp^2 network of carbon atoms, there is exactly one π^* state/atom. These states are clearly identifiable in the spectrum. Further, the lack of long-range order in C_{60} avoids some problems encountered in this type of analysis with graphite or diamond [10]. Table I summarizes the results.

The quoted uncertainties in the π^* area are based on the idea that the primary source of error is the mistaken assignment of oscillator strength near 287–289 eV, the region of the spectrum where the π^* and σ^* resonances overlap. The lower bound of the uncertainty in the π^* area is taken as the integral of the fitted π^* line shape over energies above 287 eV. Similarly, the upper bound is set to the sum of the areas under the σ_x^* and σ_c^* resonances for energies below 289 eV.

Inspection of the results for the two solids in Table I shows a higher level of π^* contributions in the a-C than in the DLC. This seems consistent with earlier estimates of 88%–100% sp^2 bonding in evaporated a-C [16,17] and with the measurements of [10] that estimate 40% of the atoms in their DLC samples are sp^2 bonded and 60% are sp^3 bonded.

For the liquids there is much more π bonding evident from the fits. The low-density untamped liquid shows 2–3 times the number of π^* states than does the a-C solid. The estimate of 2.3 π^* states/atom is close to the 2 states/atom expected for sp bonding. For the tamped liquids, we can compare to the results of the $T = 7000$ K tight-binding simulations of [5]. Values for the π^* states/atom based on

TABLE I. Summary of important results of fitting the absorption spectra. The second column lists the number of π^* states/atom estimated from the area of the π^* peak, normalized to the π^* contribution to C_{60} as described in the text. The third column lists the π^* states/atom derived from the simulation results in Fig. 2 of [5]. The quoted uncertainties in these values are based on the estimated uncertainty in the density of the target carbon ($\pm 5\%$) and on the small fraction of atomic sites in the simulation with onefold and fivefold coordination. The rightmost column gives the energy of the maximum absorption in the σ_c^* continuum feature.

Material	π^* states/site (fit)	π^*/atom (sim.)	σ_c^* peak (eV)
a-C	$0.7^{+0.2}_{-0.1}$	···	295.5 ± 0.2
DLC	$0.4^{+0.2}_{-0.1}$	···	295.6 ± 0.3
l-C, untamped	$2.3^{+0.1}_{-0.5}$	···	297.6 ± 0.9
l-C, 2.0 g/cm^3	$1.5^{+0.2}_{-0.3}$	1.5 ± 0.1	297.1 ± 0.7
l-C, 2.6 g/cm^3	$1.4^{+0.2}_{-0.3}$	1.2 ± 0.1	299.2 ± 0.9

this work are listed in Table I. These values are within 20% of the fit results for the 2.0 and 2.6 g/cm^3 liquids. The estimated values of π^* states/atom are consistent with a mixture of sp, sp^2, and sp^3 bonding at these higher liquid densities.

In the higher energy region of the spectrum, the energy of the σ_c^* continuum resonance gives a measure of the average bond length. For gas phase and adsorbed molecules, a linear correlation has been observed between the peak energy of the σ_c^* continuum resonance and bond length [18]. The σ_c^* peak energy is listed in the rightmost column of Table I. While both solids have a σ_c^* peak energy near 295.5 eV, the peak energy for the liquids is shifted to significantly higher energies. The empirical correlation between σ_c^* peak energy and bond length for small hydrocarbon molecules [18] predicts a carbon-carbon bond length of 1.45 Å for solid a-C. This result agrees well with the nearest-neighbor distance of 1.445 Å obtained from extended x-ray absorption fine structure (EXAFS) measurements [19]. Relative to the a-C solid, we estimate bond length changes of -0.04 ± 0.02 Å for the untamped liquid, -0.03 ± 0.02 Å for the 2.0 g/cm^3 liquid, and -0.07 ± 0.02 Å for the 2.6 g/cm^3 liquid. First-principles MD simulations [4] calculate 1.40 Å for the peak of the pair-correlation function at 2.76 g/cm^3 and 6000 K. This theoretical value is consistent with our measured contraction of the bond length for the 2.6 g/cm^3 liquid. It should be noted that our analysis is based on the correlation between σ_c^* resonance energy and bond length observed in molecules rather than in high temperature liquids. A broad distribution of bond lengths could itself cause a shift in the σ_c^* peak energy. A more quantitative determination of bond length would require an EXAFS measurement on liquid carbon.

This methodology of fitting the pump-probe spectra of liquid carbon provides an experimental measure of the bonding properties in the liquid as a function of density. At low densities, the liquid is predominantly sp bonded. At the higher densities attained by tamping the heated foils the fraction of sp bonded atoms is still significant, and the estimated number of π^* states/atom is close to the results of published simulations based on a tight-binding interaction model. Analysis of the peak position of the continuum resonance suggests further that the average bond length of the liquids is shorter than that of the solids, an observation consistent with the increase in π^* states. Additional theoretical work, in particular, MD simulations combined with a calculation of the absorption spectrum, could shed more light on the nature of the liquid at higher densities.

We thank J. Díaz and J. Stöhr for fruitful discussions on the interpretation of the spectra. We also thank A. Szoke and A. Cavalleri for stimulating discussions. These experiments were carried out at the Advanced Light Source, supported by the Director, Office of Science, Office of Basic Energy Sciences, Materials Sciences Division, of the U.S. Department of Energy under Contract No. DE-AC03-76SF00098 at Lawrence Berkeley National Laboratory. Additional support was provided by the U.S. Department of Energy High Energy Density Science Grants Program and the Institute for Laser Science and Applications at Lawrence Livermore National Laboratory. S. L. J. acknowledges the support of the ALS.

*Electronic address: Steve.Johnson@mailaps.org
†Current address: Stanford Synchrotron Radiation Laboratory, Menlo Park, CA 94025, USA.

[1] M. Ross, Nature (London) **292**, 435 (1981).
[2] F. P. Bundy, W. A. Bassett, M. S. Weathers, R. J. Hemley, H. K. Mao, and A. F. Goncharov, Carbon **34**, 141 (1995).
[3] A. Cavalleri, K. Sokolowski-Tinten, C. von der Linde, I. Spagnolatti, M. Bernasconi, G. Benedek, A. Podestá, and P. Milani, Europhys. Lett. **57**, 281 (2002).
[4] C. J. Wu, J. N. Glosli, G. Galli, and F. H. Ree, Phys. Rev. Lett. **89**, 135701 (2002).
[5] J. R. Morris, C. Z. Wang, and K. M. Ho, Phys. Rev. B **52**, 4138 (1995).
[6] S. L. Johnson, P. A. Heimann, A. M. Lindenberg, H. O. Jeschke, M. E. Garcia, Z. Chang, R. W. Lee, J. J. Rehr, and R. W. Falcone, Phys. Rev. Lett. **91**, 157403 (2003).
[7] K. Sokolowski-Tinten, J. Bialkowski, A. Cavalleri, and D. von der Linde, Phys. Rev. Lett. **81**, 224 (1998).
[8] S. Anders, A. Anders, I. G. Brown, B. Wei, K. Komvopoulos, J. W. Ager III, and K. M. Yu, Surf. Coat. Technol. **68/69**, 388 (1994).
[9] D. H. Reitze, H. Ahn, and M. C. Downer, Phys. Rev. B **45**, 2677 (1992).
[10] J. Díaz, S. Anders, X. Zhou, E. J. Moler, S. A. Kellar, and Z. Hussain, Phys. Rev. B **64**, 125204 (2001).
[11] J. Stöhr, *NEXAFS Spectroscopy* (Springer-Verlag, Berlin, Heidelberg, 1992).
[12] See EPAPS Document E-PRLTAO-94-029509 for the line shape of σ_c^* (appendix of the article). A direct link to this document may be found in the online article's HTML reference section. The document may also be reached via the EPAPS homepage (http://www.aip.org/pubservs/epaps.html) or from ftp.aip.org in the directory /epaps/. See the EPAPS homepage for more information.
[13] L. J. Terminello, D. K. Shuh, F. J. Himpsel, D. A. Lapiano-Smith, J. Stöhr, D. S. Bethune, and G. Meijer, Chem. Phys. Lett. **182**, 491 (1991).
[14] J. L. Solomon, R. J. Madix, and J. Stöhr, Surf. Sci. **255**, 12 (1991).
[15] To compare this spectrum with the ones collected in this study, the spectrum from [13] was scaled so that the area under the spectrum from 280 to 320 eV matched that of the a-C solid.
[16] J. Fink, T. Müller-Heinzerling, J. Pflüger, A. Bubenzer, P. Koidl, and G. Crecelius, Solid State Commun. **47**, 687 (1983).
[17] J. Fink, T. Müller-Heinzerling, J. Pflüger, B. Scheerer, B. Dischler, P. Koidl, A. Bubenzer, and R. E. Sah, Phys. Rev. B **30**, 4713 (1984).
[18] F. Sette, J. Stöhr, and A. P. Hitchcock, J. Chem. Phys. **81**, 4906 (1984).
[19] G. Comelli, J. Stöhr, C. J. Robinson, and W. Jark, Phys. Rev. B **38**, 7511 (1988).